AMERICAN SOCIETY FOR MICROBIOLOGY | Antimicrobial Agents and Chemotherapy®

PHARMACOLOGY

Antischistosomiasis Liver Fibrosis Effects of Chlorogenic Acid through IL-13/miR-21/Smad7 Signaling Interactions *In Vivo* and *In Vitro*

Yao Wang,[a] Fan Yang,[b] Jun Xue,[c] Xuan Zhou,[d] Lei Luo,[a] Qian Ma,[e] Yun-Fei Chen,[f] Juan Zhang,[a] Shu-Ling Zhang,[d] Lei Zhao[d]

School of Clinical Medicine, Hubei University of Chinese Medicine, Wuhan, People's Republic of China[a]; Department of Hepatology, Hubei Provincial Hospital of Chinese Medicine, Wuhan, People's Republic of China[b]; Cancer Center, Union Hospital, Tongji Medical College, Huazhong University of Science and Technology, Wuhan, People's Republic of China[c]; Department of Infectious Diseases, Union Hospital, Tongji Medical College, Huazhong University of Science and Technology, Wuhan, People's Republic of China[d]; School of Life Science, Hubei University, Wuhan, People's Republic of China[e]; Department of Vascular Surgery, Union Hospital, Tongji Medical College, Huazhong University of Science and Technology, Wuhan, People's Republic of China[f]

ABSTRACT This study investigated the antischistosomiasis liver fibrosis effects of chlorogenic acid (CGA) on interleukin 13 (IL-13)/microRNA-21 (miR-21)/Smad7 signaling interactions in the hepatic stellate LX2 cell line and schistosome-infected mice. The transfection was based on the ability of the GV273–miR-21–enhanced green fluorescent protein (EGFP) and GV369–miR-21–EGFP lentiviral system to up- or down-regulate the miR-21 gene in LX2 cells. The mRNA expression of miR-21, Smad7, and connective tissue growth factor (CTGF) and the protein expression of Smad7, CTGF, Smad1, phosphor-Smad1 (p-Smad1), Smad2, p-Smad2, Smad2/3, p-Smad2/3, transforming growth factor β (TGF-β) receptor I, and α-smooth muscle actin (α-SMA) was assayed. Pathological manifestation of hepatic tissue was assessed for the degree of liver fibrosis in animals. The results showed that CGA could inhibit the mRNA expression of miR-21, promote Smad7, and inhibit CTGF mRNA expression. Meanwhile, CGA could significantly lower the protein levels of CTGF, p-Smad1, p-Smad2, p-Smad2/3, TGF-β receptor I, and α-SMA and elevate the Smad7 protein level. *In vivo*, with treatment with CGA, the signaling molecules of IL-13/miR-21/Smad7 interactions were markedly regulated. CGA could also reduce the degree of liver fibrosis in pathological manifestations. In conclusion, CGA could inhibit schistosomiasis-induced hepatic fibrosis through IL-13/miR-21/Smad7 signaling interactions in LX2 cells and schistosome-infected mice and might serve as an antifibrosis agent for treating schistosomiasis liver fibrosis.

KEYWORDS chlorogenic acid, schistosomiasis, liver fibrosis, IL-13, miR-21, Smad7

According to conservative estimates, schistosomiasis is an infectious disease that affects more than 230 million people in more than 70 countries (1, 2). There are currently at least 600 million people at risk worldwide, and the number of deaths due to schistosomiasis is approximately 200,000 each year (3). Schistosomiasis japonica is still the biggest threat to the Chinese public; the number of patients is about 360,000, and the cost of prevention and control is up to $120 million every year (4).

Praziquantel is currently the only clinically effective drug for the treatment of schistosomiasis since the 1980s. However, there have been isolated reports of less sensitive parasites belonging to strains that were selected in the laboratory for that phenotype (5). Adult worms (days 35 to 42) are the most susceptible to praziquantel,

Received 24 June 2016 **Returned for modification** 4 September 2016 **Accepted** 17 November 2016

Accepted manuscript posted online 21 November 2016

Citation Wang Y, Yang F, Xue J, Zhou X, Luo L, Ma Q, Chen Y-F, Zhang J, Zhang S-L, Zhao L. 2017. Antischistosomiasis liver fibrosis effects of chlorogenic acid through IL-13/miR-21/Smad7 signaling interactions *in vivo* and *in vitro*. Antimicrob Agents Chemother 61:e01347-16. https://doi.org/10.1128/AAC.01347-16.

Address correspondence to Lei Zhao, leizhao@hust.edu.cn.

Y.W., F.Y., and J.X. contributed equally to this study.

but the early stages of schistosomula (days 0 to 7) are particularly resistant to tegument damage, and the eggs of schistosomes are not sensitive. In schistosomiasis, eggs are the main cause of pathology. *Schistosoma* eggs release soluble egg antigen (SEA) (6), and the SEA stimulates the body to produce interleukin 13 (IL-13), which combines with receptors on hepatic stellate cells to switch on Smad1/2 (the abbreviation of Smad1/5 and Smad2/3) molecule phosphorylation, leading to liver fibrosis (7). In the signaling interactions, microRNA-21 (miR-21) positively regulates the production of collagen via Smad1/2 (Smad1/5 and Smad2/3) phosphorylation and is interfered with by Smad7 (8). Thus, the interaction between IL-13, miR-21, and Smad7 molecules in hepatic stellate cells can ultimately induce the production of collagen and schistosomiasis liver fibrosis.

Chlorogenic acid (CGA) (5-caffeoylquinic acid) is the ester of caffeic acid and quinic acid (9, 10) and is an important biosynthetic intermediate that has been discovered in a number of dietary plants and medicinal herbs, such as bamboo (*Phyllostachys edulis*) (11). The molecular formula is $C_{16}H_{18}O_9$ (12). It has been reported that CGA has strong anti-inflammatory (13), antioxidative (14, 15), antihypertensive (16), antitumor (17, 18), and analgesic and antipyretic (19, 20) effects. In addition, CGA could inhibit lipopolysaccharide (LPS)-induced microglial activation and improve the survival of dopaminergic neurons (21). CGA could also reduce carbon tetrachloride-induced liver fibrosis in rats through inhibition of the Toll-like receptor 4 signaling pathway (22, 23) and through the suppression of oxidative stress in liver and hepatic stellate cells (24).

However, the molecular mechanism through which CGA inhibits liver fibrosis in hepatic stellate cells remains unknown. The objective of this study is to confirm whether CGA can inhibit schistosomiasis-induced liver fibrosis through IL-13/miR-21/Smad7 signaling interactions in hepatic satellite cells (HSCs) and schistosome-infected mice.

RESULTS

Cytotoxicity of CGA on LX2 cells. Based on the cell-counting kit 8 (CCK8) assay, pretreatment of unstimulated LX2 cells with prepared solutions of 80 μg/ml, 40 μg/ml, and 20 μg/ml of CGA for 24 h did not significantly affect cell viability (Fig. 1A). Observation of cell morphology showed the same result (Fig. 1B). Furthermore, in assays by real-time PCR, the difference between changes of miR-21 in CGA-treated cells and the control group was not significant (Fig. 1C). Therefore, we chose CGA at 80 μg/ml, 40 μg/ml, and 20 μg/ml to treat cells for 24 h.

IL-13 induces CTGF protein expression in LX2 cells. There was a time- and dosage-dependent increase in the expression of connective tissue growth factor (CTGF) protein in LX2 cells treated with IL-13 (Fig. 2). The effect of IL-13 on CTGF expression was dose dependent over the range of 5 to 100 ng/ml after 6-h treatment (Fig. 2A and B). An approximately 1-fold increase in the CTGF protein level was observed at 6 h after IL-13 treatment (Fig. 2C and D). IL-13 at 50 ng/ml significantly increased CTGF expression ($P < 0.01$), and this concentration was chosen for subsequent experiments. IL-13 at 50 ng/ml significantly increased the expression of miR-21 mRNA after 6 h (Fig. 2E and F), when the 0-ng/ml group was compared with the 50-ng/ml group after the cells were stimulated with IL-13 for 6 h ($P < 0.01$) and when the 0-h group was compared with the 6-h group after the cells were stimulated with IL-15 at a concentration of 50 ng/ml ($P < 0.01$).

Effect of CGA on miR-21 and downstream molecules in LX2 cells after IL-13 stimulation. As shown in Fig. 3A, compared with the control group, the mRNA levels of miR-21 and CTGF in the experimental group were significantly increased ($P < 0.01$) and the level of Smad7 was significantly decreased ($P < 0.01$). After treatment with CGA at different concentrations for 24 h, the levels of miR-21 and CTGF were decreased and the level of Smad7 was increased compared with the experimental group ($P < 0.05$ or 0.01). As shown in Fig. 3B, the protein levels were also assessed by Western blot analysis. IL-13 markedly elevated the expression of CTGF, phosphorylated Smad1 (p-Smad1), p-Smad2, p-Smad2/3, transforming growth factor β (TGF-β) receptor I, and α-smooth muscle actin (α-SMA) and lowered the level of Smad7 in IL-13-stimulated

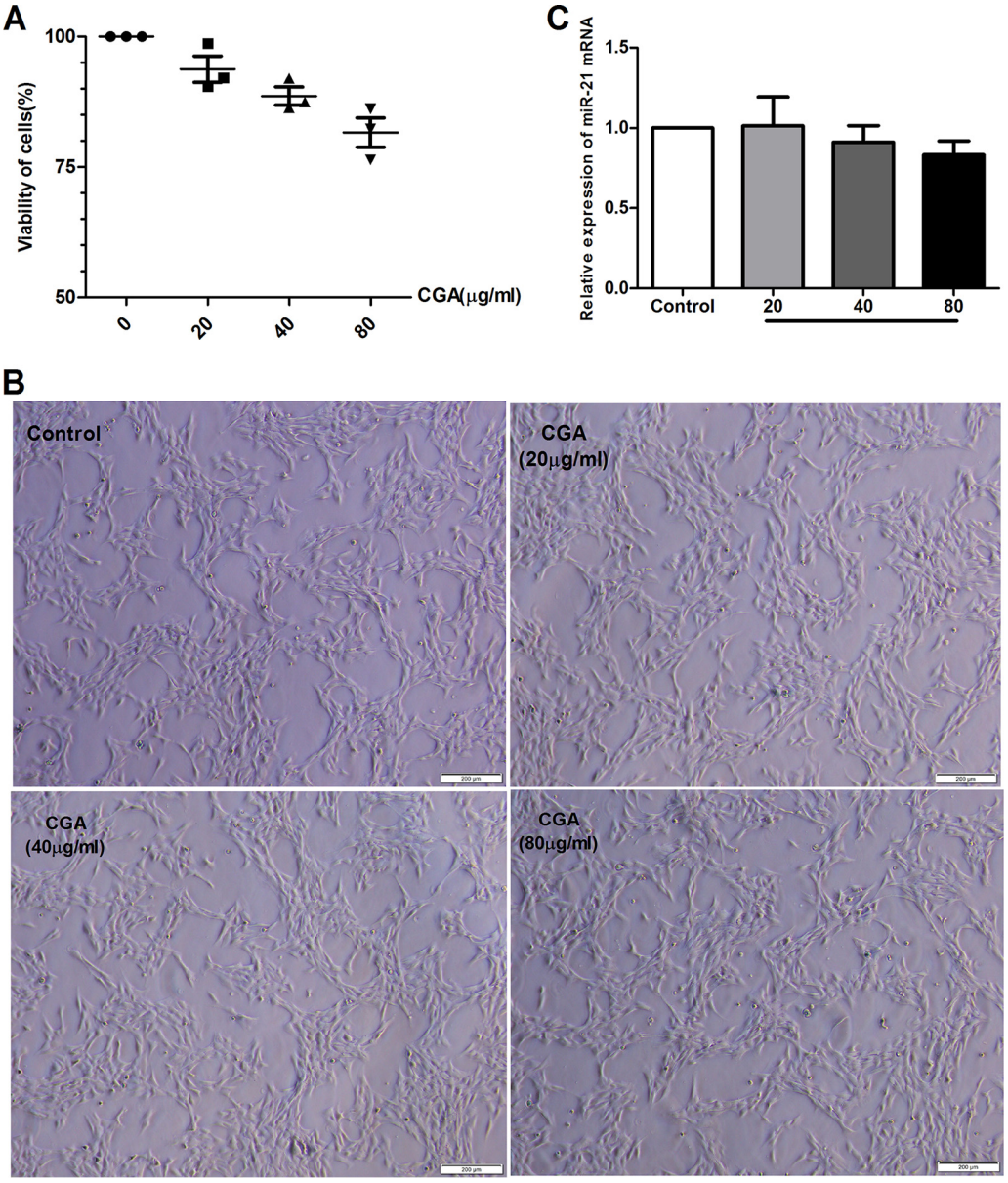

FIG 1 Cytotoxicity of CGA on LX2 cells. (A) CCK8 assay of LX2 viability after CGA treatment. (B) Morphologies of LX2 cells after CGA treatment for 24 h. (C) mRNA levels measured by quantitative real-time PCR. The data are shown as means and SEM.

cells. However, IL-13-induced p-Smad1, p-Smad2, p-Smad2/3, TGF-β receptor I, CTGF, and α-SMA expression was effectively inhibited by CGA, and CGA could promote Smad7 expression compared with the experimental group. The total Smad1, Smad2, and Smad2/3 levels showed no significant changes.

Expression of downstream signaling molecules in LX2 cells after miR-21 knockdown. We constructed the miR-21 lentiviral vector GV273 and transfected LX2 cells *in vitro*. Green fluorescent protein (GFP) was observed with a fluorescence microscope after 48 h and 72 h (Fig. 4A), and the expression of miR-21, Smad7, and CTGF was confirmed (Fig. 4B). At 72 h after transfection, we observed the impact of miR-21/Smad7 signaling interactions on molecules downstream. There was no significant difference between the control group and the lentivirus negative-control (lentivirus-NC) group in the mRNA levels of miR-21, Smad7, and CTGF ($P > 0.05$) (Fig. 4B) and the protein levels of CTGF, Smad7, p-Smad1, p-Smad2, p-Smad2/3, and TGF-β receptor I (Fig. 4C). However, compared with the control group, after miR-21 knockdown, the mRNA

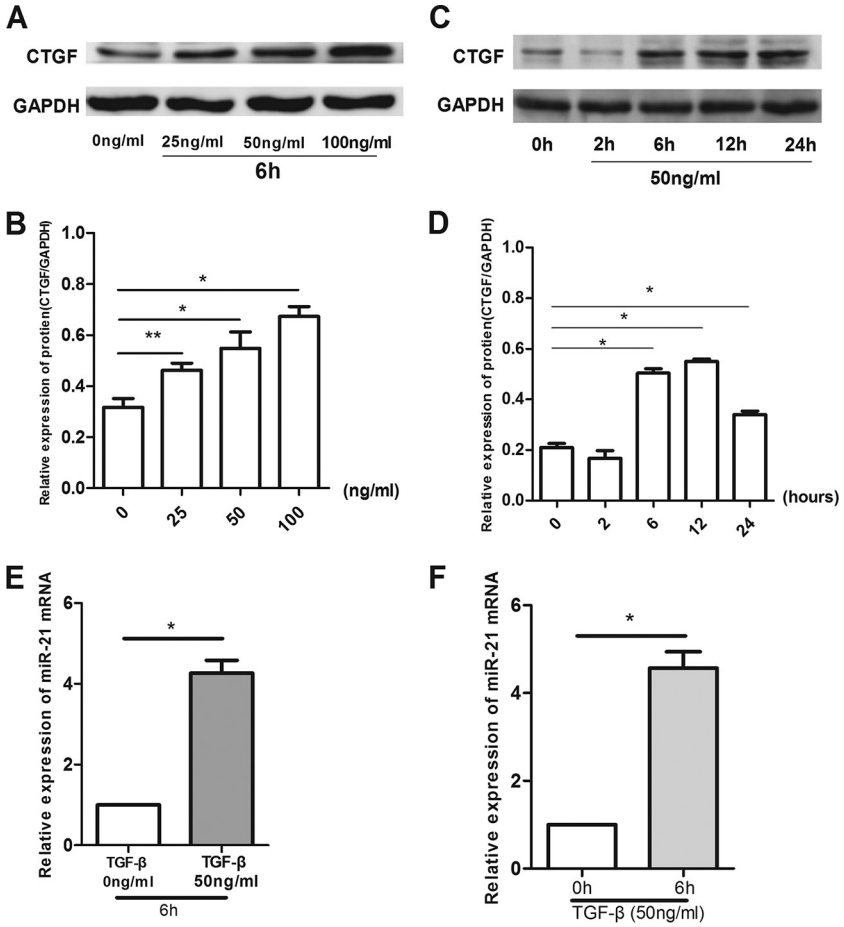

FIG 2 There was a time- and dose-dependent increase in the expression of CTGF protein in LX2 cells treated with IL-13. (A and B) The protein levels were assayed by Western blotting. The effect of IL-13 on CTGF expression was dose dependent over the range of 5 to 100 ng/ml after 6 h treatment. *, $P < 0.01$ compared with the 0-ng/ml group; **, $P < 0.05$ compared with the 0-ng/ml group. (C and D) The CTGF protein level increased with IL-13 treatment after 6 h. *, $P < 0.01$ compared with the 0-h group. (E and F) mRNA levels were measured by real-time PCR. IL-13 at 50 ng/ml after 6 h significantly increased the expression of miR-21 mRNA. *, $P < 0.01$ for 0 ng/ml versus 50 ng/ml or 0 h versus 6 h. The data are shown as means and SEM of the results of three independent experiments, each performed in duplicate.

expression of miR-21 and CTGF decreased and the level of Smad7 increased ($P < 0.01$) (Fig. 4B). The protein expression of CTGF, p-Smad1, p-Smad2, p-Smad2/3, and TGF-β receptor I decreased, and the level of Smad7 increased (Fig. 4C).

Effect of CGA on downstream signaling molecules in LX2 cells after miR-21 knockdown. MiR-21 was knocked down by lentiviral vector in LX2 cells for 72 h, and then the cells were treated with CGA (80 μg/ml) for 24 h. The LX2 cells were treated with IL-13 for the last 6 h before harvest. Compared with the lentivirus-down group (where miR-21 was knocked down in the LX2 cells by a lentiviral vector), the mRNA levels of miR-21 and CTGF in the lentivirus-down/IL-13 group were increased ($P < 0.01$) and the level of Smad7 was decreased ($P < 0.01$) (Fig. 5A), and the protein expression of CTGF, p-Smad1, p-Smad2, p-Smad2/3, and TGF-β receptor I increased and the level of Smad7 decreased (Fig. 5B). When LX2 cells were treated with CGA (80 μg/ml), the level of miR-21 and CTGF were decreased compared to that in the lentivirus-down/IL-13 group ($P < 0.05$ or 0.01) and the level of Smad7 increased ($P < 0.01$) (Fig. 5A). The protein levels of CTGF, p-Smad1, p-Smad2, p-Smad2/3, and TGF-β receptor I decreased, and the level of Smad7 increased (Fig. 5B).

Expression of downstream signaling molecules in LX2 cells after miR-21 overexpression. We constructed the miR-21 lentiviral vector GV369 and transfected LX2

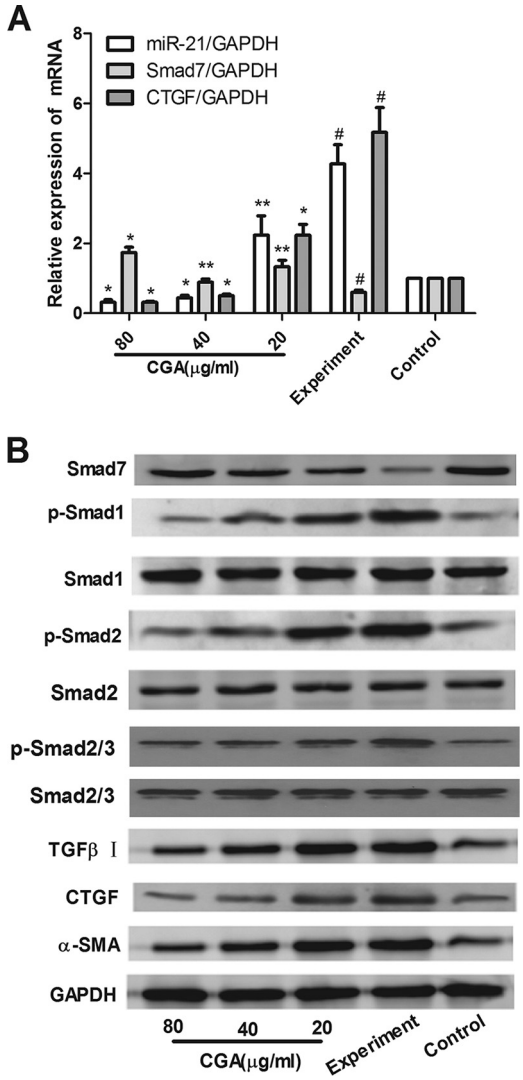

FIG 3 Effects of CGA on IL-13/miR-21/Smad7 interactions in LX2 cells after IL-13 stimulation. The mRNA levels were measured by real-time PCR. (A) mRNA levels of miR-21 and CTGF in the experimental group were increased and the level of Smad7 was decreased. (B) Protein levels were assayed by Western blotting. CGA was administered at different concentrations for 24 h, and IL-13 markedly increased the expression of CTGF, p-Smad1, p-Smad2, p-Smad2/3, TGF-β receptor I, and α-SMA and decreased the level of Smad7 in IL-13-stimulated cells. However, IL-13-induced p-Smad1, p-Smad2, p-Smad2/3, TGF-β receptor I, CTGF, and α-SMA expression was effectively inhibited by CGA, and CGA could promote Smad7 expression. Total Smad1, Smad2, and Smad2/3 showed no significant changes. The data are shown as means and SEM of the results of three independent experiments, each performed in duplicate. *, $P < 0.01$ compared with the experimental group; **, $P < 0.05$ compared with the experimental group; #, $P < 0.01$ compared with the control group.

cells *in vitro*. GFP was observed with a fluorescence microscope after 48 h and 72 h (Fig. 6A), and the expression of miR-21 was confirmed (Fig. 6B). At 72 h after transfection, we observed the impact of miR-21/Smad7 signaling interactions on molecules downstream. There was no significant difference between the control and lentivirus-NC groups in the mRNA levels of miR-21, Smad7, and CTGF ($P > 0.05$) (Fig. 6B) and the protein levels of CTGF, Smad7, p-Smad1, p-Smad2, p-Smad2/3, and TGF-β receptor I (Fig. 6C). However, compared with the control group, after miR-21 overexpression, the mRNA expression of miR-21 and CTGF increased and the level of Smad7 decreased ($P < 0.01$) (Fig. 6B). The protein expression of CTGF, p-Smad1, p-Smad2, p-Smad2/3, and TGF-β receptor I increased, and the level of Smad7 decreased (Fig. 6C).

Effect of CGA on downstream signaling molecules in LX2 cells after miR-21 overexpression. After being treated with CGA (80 μg/ml) for 24 h after miR-21

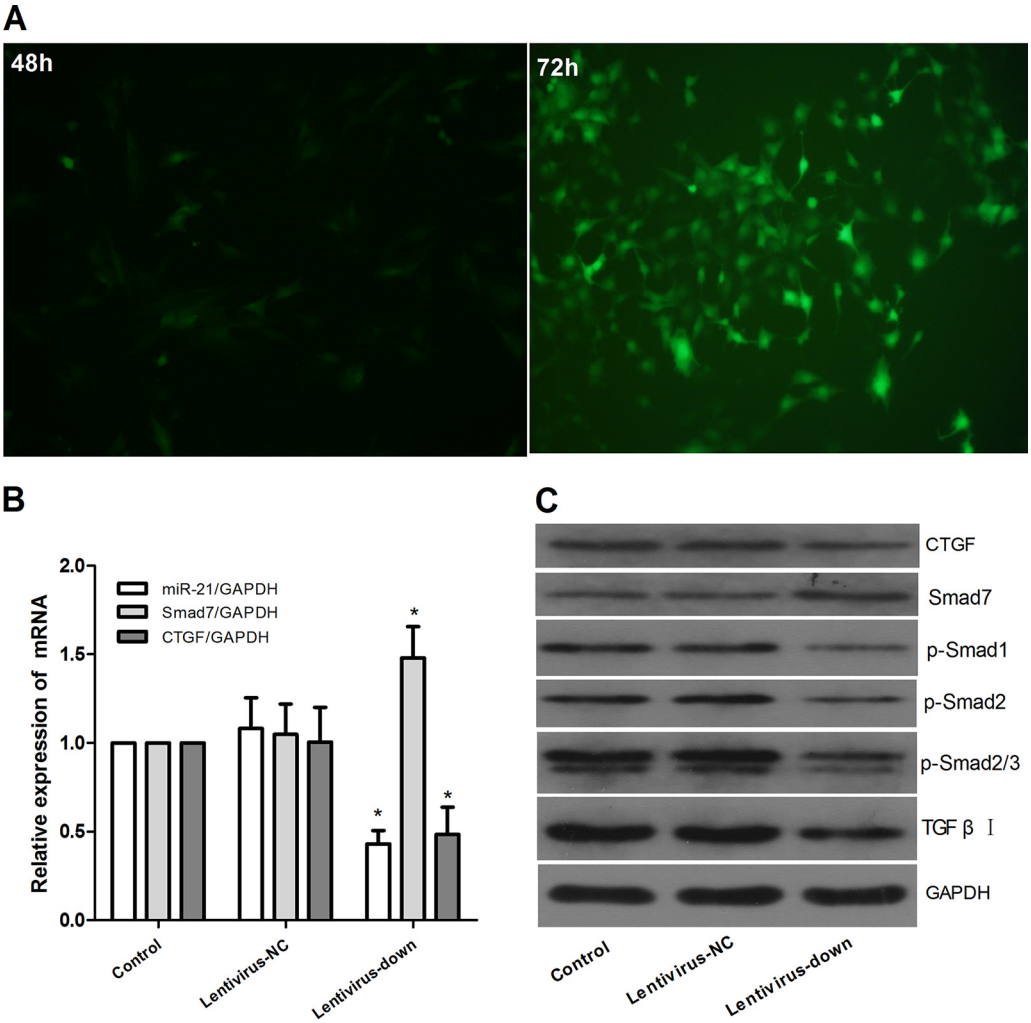

FIG 4 Downregulation of miR-21 in LX2 cells via the lentiviral vector. The lentiviral vector interfered with LX2 cells for 72 h to mediate miR-21 down expression. (A) The expression of GFP was observed with a fluorescence microscope after lentivirus was introduced into LX2 cells for 48 and 72 h. (B) Expression of miR-21, Smad7, and CTGF was detected by quantitative real-time PCR. (C) Expression of protein was assayed by Western blotting. The data are shown as means and SEM; $n = 3$. *, $P < 0.01$ for lentivirus-down versus control groups, a significant difference from the respective values determined by ANOVA.

overexpression, the LX2 cells were treated with IL-13 for the last 6 h before harvest. As shown in Fig. 7A, compared with the lentivirus-up group (where miR-21 was overexpressed in LX2 cells by a lentiviral vector), the mRNA levels of miR-21 and CTGF in the lentivirus-up/IL-13 group were increased ($P < 0.01$) and the level of Smad7 was decreased ($P < 0.01$), and the protein expression of CTGF, p-Smad1, p-Smad2, p-Smad2/3, and TGF-β receptor I increased and the level of Smad7 decreased (Fig. 7B). When the LX2 cells were treated with CGA (80 μg/ml), the levels of miR-21 and CTGF were decreased compared to that in the lentivirus-up/IL-13 group ($P < 0.05$ or 0.01) and the level of Smad7 increased ($P < 0.01$, Fig. 7A), and the protein levels of CTGF, p-Smad1, p-Smad2, p-Smad2/3, and TGF-β receptor I decreased and the level of Smad7 increased (Fig. 7B).

Effect of CGA on egg numbers and IL-13. As hepatic fibrosis is mainly induced by SEA secreted from the eggs of schistosomes (Fig. 8C), the eggs in infected mouse livers were important for the experiment. The numbers of eggs in the control and CGA groups were not significantly different ($P > 0.05$) (data not shown). As illustrated in Fig. 8C, the level of IL-13 was increased in the experimental group compared with the control group ($P < 0.01$) and was significantly decreased in a concentration-dependent

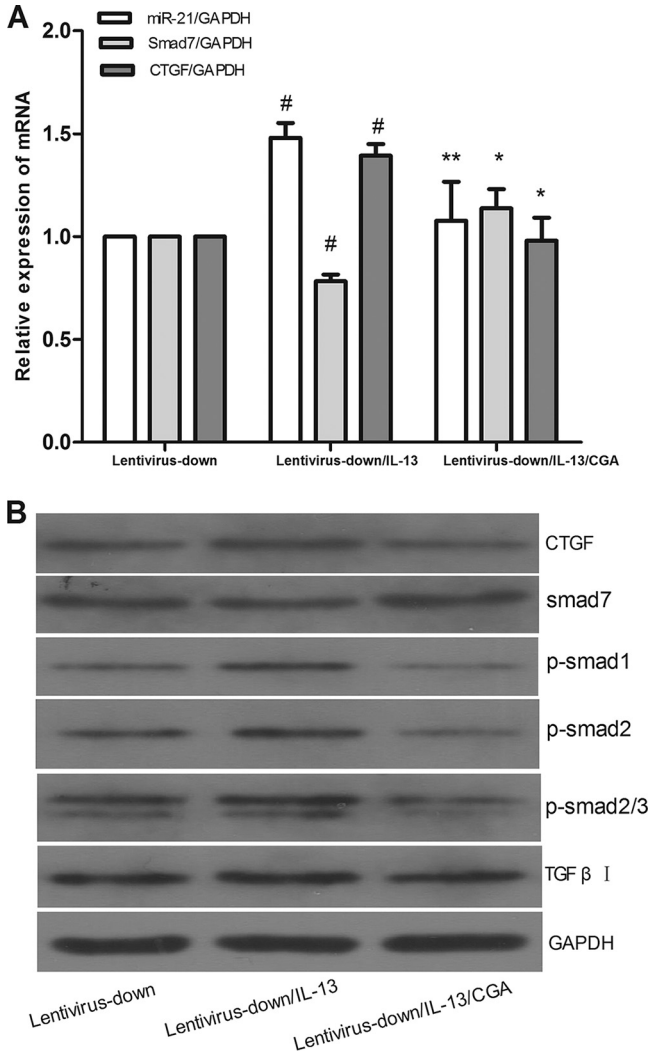

FIG 5 Lentivirus vector interfered with LX2 cells for 72 h to mediate miR-21 down expression, and then the cells were treated with CGA (80 μg/ml) for 24 h. Then, the LX2 cells were treated with IL-13 for the last 6 h before harvest. (A) mRNA levels were measured by quantitative real-time PCR. (B) Protein levels were measured by Western blotting. The data are shown as means and SEM; $n = 3$. #, $P < 0.01$ for lentivirus-down/IL-13 versus lentivirus-down; *, $P < 0.01$ for lentivirus-down/IL-13/CGA versus lentivirus-down/IL-13; **, $P < 0.01$ for lentivirus-down/IL-13/CGA versus lentivirus-down/IL-13, significant differences from the respective values determined by Student's *t* test.

manner by treatment with CGA ($P < 0.05$). These findings suggested that CGA negatively regulated the level of IL-13.

Pathological manifestation of hepatic tissue. As illustrated in Fig. 8A, nodules on liver surfaces in the experimental group could be clearly observed. The mice that were treated with different concentrations of CGA exhibited reduced nodules. In order to evaluate the antifibrosis role of CGA *in vivo*, histological analysis with hematoxylin and eosin (H&E) and Sirius red was used to gauge the extent of liver injury induced by schistosomes (Fig. 8E). Under a light microscope, the slice of liver from the control group showed that the structure of hepatic lobules was obviously intact, with orderly arranged liver cells, and there were no egg granulomas, no cell denaturation, no infiltration of inflammatory cells, and no fibrillary collagens. In the experimental group, the liver cells were severely damaged and showed vacuolar change, and significant deposition of fibrillary collagens was also detected. Enormous egg granulomas were surrounded by accumulation of inflammatory cells and fibril aggregation. In contrast, in the CGA group, the slice showed smaller granulomas, less liver cell denaturation, less

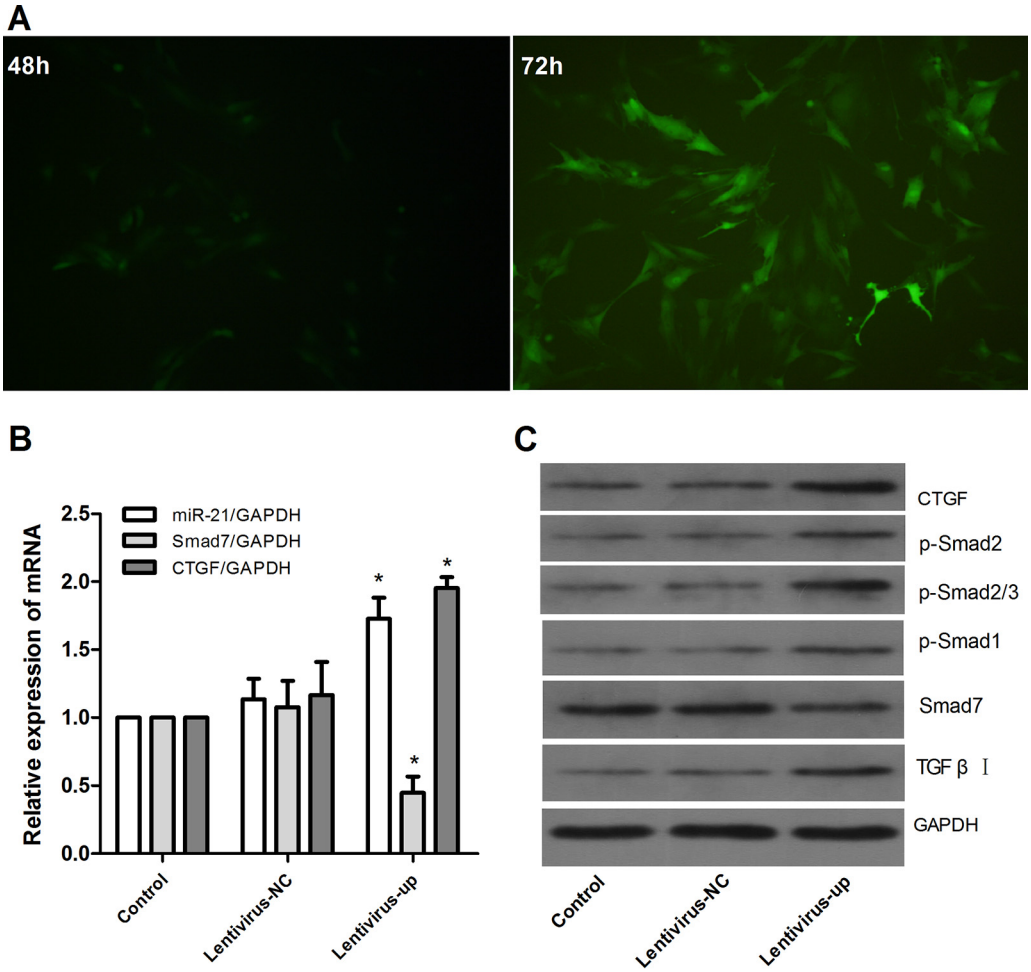

FIG 6 Upregulation of miR-21 in LX2 cells via the lentiviral vector. The lentiviral vector interfered with LX2 cells for 72 h to mediate miR-21 overexpression. (A) Expression of GFP was observed with a fluorescence microscope after lentivirus was introduced into LX2 cells for 48 and 72 h. (B) Expression of miR-21, Smad7, and CTGF was detected by quantitative real-time PCR. (C) Expression of protein was assayed by Western blotting. The data are shown as means and SEM; $n = 3$. *, $P < 0.01$ for lentivirus-up versus control, a significant difference from the respective values determined by ANOVA.

inflammatory cell infiltration, and less fibrillary collagen. The connective tissues were obviously decreased.

Protein expression of α-SMA examined by immunohistochemistry (IHC) in schistosome-infected mice. As shown in Fig. 8F, in the control group, the staining of α-SMA in the cytoplasm was not remarkable. After infection with schistosomes, the positivity rate of α-SMA staining in the cytoplasm rose significantly ($P < 0.01$). With CGA treatment, the rate of α-SMA staining in the cytoplasm was markedly decreased ($P <$ 0.05 or 0.01).

Effect of CGA on IL-13/miR-21/Smad7 signaling interactions in schistosome-infected mice. As shown in Fig. 9A, compared with the control group, the mRNA levels of miR-21 and CTGF in the experimental group were significantly increased ($P < 0.01$) and the level of Smad7 was significantly decreased ($P < 0.01$). After treatment with CGA at different concentrations for 24 h, the levels of miR-21 and CTGF were decreased and the level of Smad7 was decreased compared to those in the experimental group ($P <$ 0.05 or 0.01). As shown in Fig. 9B, protein levels were also assessed by Western blot analysis. The protein expression levels of CTGF, p-Smad1, p-Smad2, p-Smad2/3, TGF-β receptor I, and α-SMA were markedly increased, and the level of Smad7 in the experimental group was decreased compared with the control group. However, the schistosome-induced protein expression of p-Smad1, p-Smad2, p-Smad2/3, TGF-β

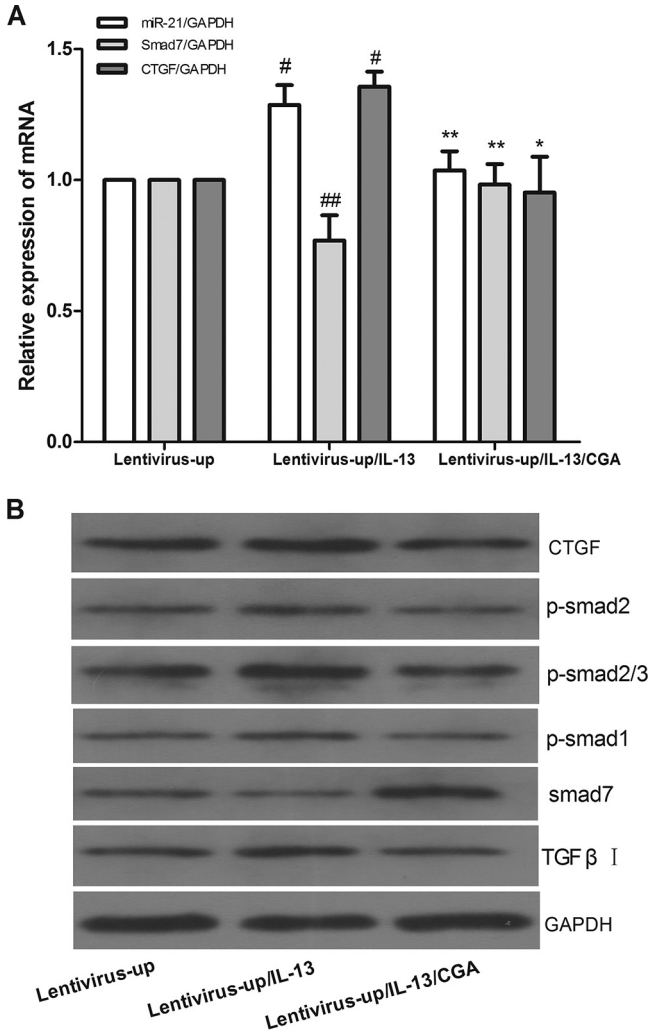

FIG 7 Lentivirus vector interfered with LX2 cells for 72 h to mediate miR-21 overexpression, and then the cells were treated with CGA (80 μg/ml) for 24 h. Then, the LX2 cells were treated with IL-13 for the last 6 h before harvest. (A) mRNA levels were measured by quantitative real-time PCR. (B) Protein levels were measured by Western blotting. The data were expressed as means and SEM; $n = 3$. #, $P < 0.01$ for lentivirus-up/IL-13 versus lentivirus-up; *, $P < 0.01$ for lentivirus-up/IL-13/CGA versus lentivirus-up/IL-13; **, $P < 0.01$ for lentivirus-up/IL-13/CGA versus lentivirus-up/IL-13, significant differences from the respective values determined by Student's *t* test; ##, $P < 0.05$ for lentivirus-up/IL-13 versus lentivirus-up.

receptor I, CTGF, and α-SMA was effectively inhibited by CGA, and CGA could promote Smad7 expression compared with the experimental group. The protein levels of Smad1, Smad2, and Smad2/3 showed no significant changes.

DISCUSSION

Schistosomiasis-induced liver fibrosis is mainly caused by SEA, an antigen that induces the production of IL-13 (but not TGF-β) as a starting signal (25). IL-13 combines with the receptors (IL-13Rα1/IL-4Rα) on hepatic stellate cells, and then the JAK-STAT6 pathway and the M2 macrophage alternative activation pathway are activated, with excess collagen deposition (26). However, simply blocking the two pathways cannot completely prevent the development of liver fibrosis.

Researchers have found that the IL-13/miR-21/Smad7 signaling interactions in hepatic stellate cells are equally important in the two signaling pathways that can influence the formation of collagen and play an important role in the development of schistosome-induced hepatic fibrosis (27). The receptors (IL-13Rα1/IL-4Rα) on hepatic stellate cells were stimulated by IL-13 through Smad1/2 (Smad1/5 and Smad2/3)

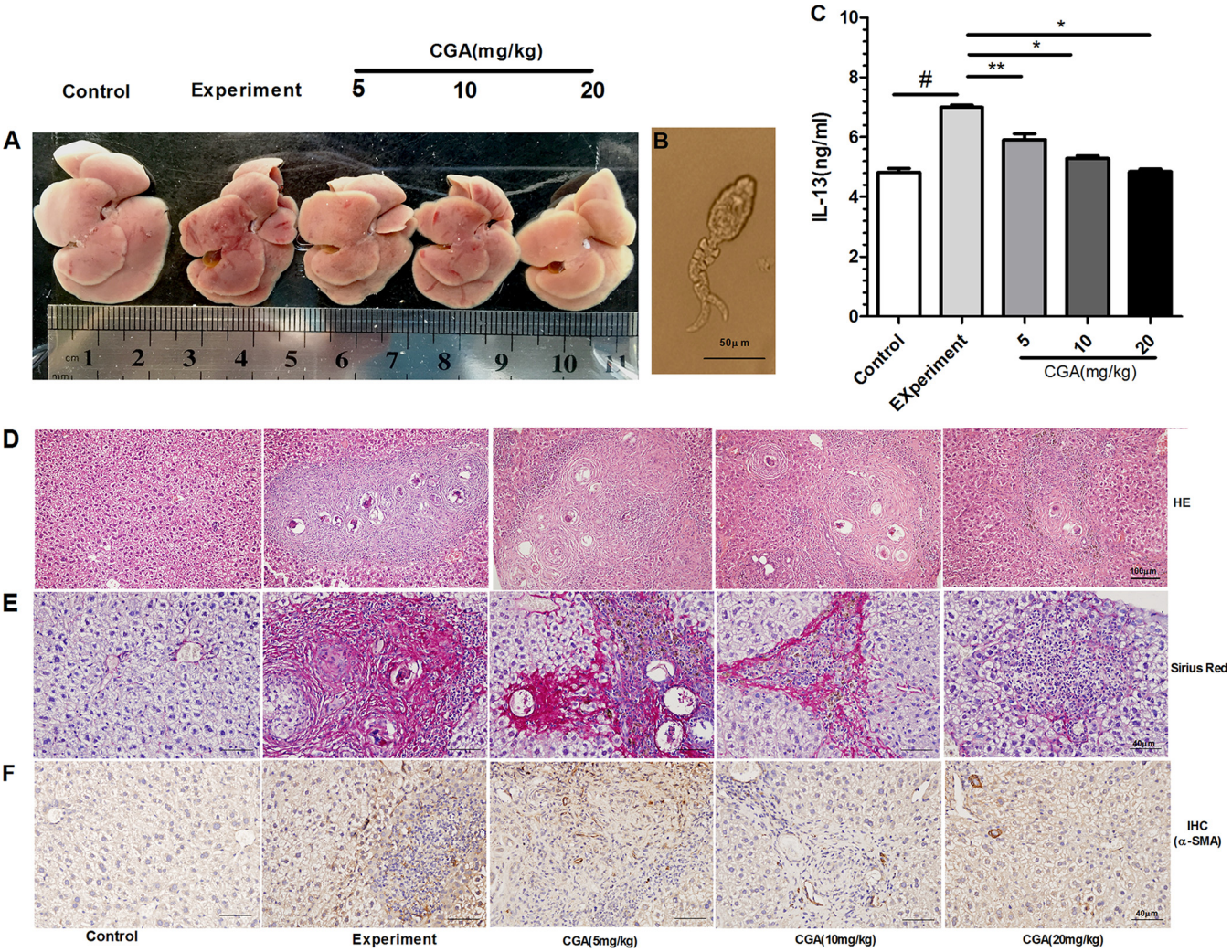

FIG 8 (A) Nodules on the liver surface could be clearly observed in the experimental group, and livers that were treated with different concentrations of CGA exhibited reduced nodules. (B) *S. japonicum* cercaria at ×400 magnification under a light microscope (used to infect mice by the abdominal-patch method). (C) IL-13 levels in sera as determined by ELISA. (D) H&E staining at ×200 magnification. (E) Sirius red staining at ×400 magnification. (F) The effects of CGA on CTGF expression were examined by immunohistochemistry. The optical densities in the images were analyzed with IPP software. After schistosome infection, the rate of α-SMA positivity significantly increased in the experimental group compared with the control group ($P < 0.01$), and CGA treatment markedly decreased the rate of α-SMA positivity compared with the experimental group ($P < 0.05$ or 0.01). *, $P < 0.01$ compared with the experimental group; **, $P < 0.05$ compared with the experimental group; #, $P < 0.01$ compared with the control group, as determined by Student's *t* test.

phosphorylation (7), positively regulating production of miR-21 and then interfering with the target genes of miR-21 and Smad7 and subsequently preventing Smad7 from negative-feedback regulation of Smad1/2 (Smad1/5 and Smad2/3). Thus, by forming a feedback loop, the molecules promote hepatic stellate cell production of collagen. The feedback loop starting from miR-21 plays a core role in the gradually increased IL-13/Smad signaling pathway (28). CTGF, synthesized by hepatocytes and HSCs (29), is a fibrogenic master switch in the epithelial-to-mesenchymal-cell transition and plays an important role in the increase of extracellular matrix (ECM) (30). The production of CTGF was closely related to the IL-13/Smad pathway (Fig. 10). Therefore, approaches to regulate the IL-13/miR-21/Smad7 interactions in the chronic stage of schistosome infection will be able to control the development of schistosomiasis liver fibrosis.

As a key activator of HSCs, TGF-β receptor I can upregulate the proteins associated with ECM and cellular receptors of several matrix proteins (31) to further promote hepatocyte injury and death, as well as the deposition of ECM components in the liver (32). In response to liver injury, quiescent HSCs undergo phenotypic alterations, en-

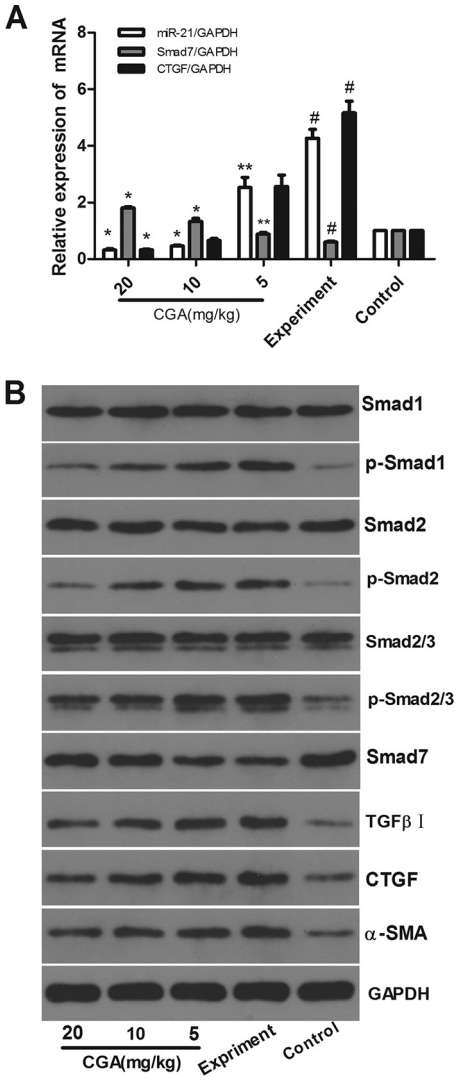

FIG 9 Effects of CGA on IL-13/miR-21/Smad7 interactions in schistosome-infected mice. The mRNA levels were measured by real-time PCR. (A) mRNA levels of miR-21 and CTGF in the experimental group increased, and the level of Smad7 decreased. (B) Protein levels were assayed by Western blotting. With administration of CGA at different concentrations for 24 h, the expression levels of CTGF, p-Smad1, p-Smad2, p-Smad2/3, TGF-β receptor I, and α-SMA were markedly increased, and the level of Smad7 was decreased in the experimental group. The expression of p-Smad1, p-Smad2, p-Smad2/3, TGF-β receptor I, CTGF, and α-SMA was effectively inhibited by CGA, and CGA could promote Smad7 expression compared with the experimental group. Total Smad1, Smad2, and Smad2/3 showed no significant changes. The data are shown as means and SEM of the results of three independent experiments, each performed in duplicate. *, $P < 0.01$ compared with the experimental group; **, $P < 0.05$ compared with the experimental group; #, $P < 0.01$ compared with the control group.

hancing cell proliferation and expression of α-SMA (33). Along with fibrogenic stimulation, HSCs lose their retinoid stores and proliferate and express excess α-SMA.

MicroRNA-21 was the first miRNA molecule discovered and confirmed in mammals. Experiments have shown that miR-21 has a significant impact on the formation and development of tumors and cardiovascular diseases (34, 35). In different diseases, miR-21 regulates signals differently. This study found that TGF-β, JAK, STAT, and other molecules can induce miR-21 regulation signals in different diseases, and these molecules are also related to hepatic fibrosis (36, 37). Whether miR-21 directly regulates the occurrence and development of hepatic fibrosis of schistosomiasis in hepatic stellate cells is worthy of further study. Therefore, we regulated miR-21 up or down by lentiviral transfection and researched the specific regulatory mechanisms of CGA. The changes in

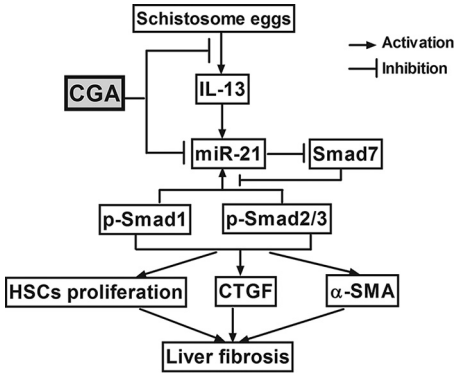

FIG 10 Diagram of CGA protection against schistosomiasis liver fibrosis *in vivo* and *in vitro* by regulating IL-13/miR-21/Smad7 signaling interactions.

miR-21 up- or downregulation will help to discover how CGA influences signaling interactions through miR-21.

In our study, the levels of miR-21, p-Smad1, p-Smad2, p-Smad2/3, TGF-β receptor I, CTGF, and α-SMA increased and Smad7 decreased significantly in the experimental group, and there was no obvious change in Smad1 and Smad2 levels. Whether in miR-21-upregulated or miR-21-downregulated LX2 cells, IL-13/miR-21/Smad7 signaling interactions could be activated after stimulation by IL-13 in the experimental group. After treatment with CGA in miR-21-up- or -downregulated LX2 cells, the IL-13/miR-21 signaling interactions for liver fibrosis were markedly inhibited. CGA could inhibit the mRNA expression of miR-21 and promote Smad7 and inhibit CTGF mRNA expression. Meanwhile, CGA could significantly reduce the protein levels of CTGF, p-Smad1, p-Smad2, p-Smad2/3, TGF-β receptor I, and α-SMA and promote the Smad7 protein level. Furthermore, in order to investigate the effect of CGA on IL-13/miR-21/Smad7 signaling interactions in schistosome-infected mice, we established an animal model of schistosomiasis-induced liver fibrosis and then treatment with CGA. In the process of creating a mouse model, in order to kill adult schistosomes, it is worth noting that we used 5 days of praziquantel administration alone after 4 weeks of modeling. Lastly, the mice of the experimental and control groups were administered normal saline, and the mice in the CGA groups were administered different concentrations of CGA. The numbers of eggs in the experimental and CGA groups were not significantly changed. CGA could reduce the degree of liver fibrosis in pathological manifestation. The level of IL-13 was increased in the experimental group, and CGA could significantly decrease the serum IL-13 concentration. The results were the same in cellular and animal models, where the IL-13/miR-21/Smad7 signaling interactions were activated in mice with schistosomiasis hepatic fibrosis, and with treatment with CGA, liver fibrosis was markedly inhibited by regulating IL-13/miR-21/Smad7 interactions (Fig. 10).

In summary, we investigated the efficacy of CGA in regulating IL-13/miR-21/Smad7 signaling interactions to suppress hepatic fibrosis *in vivo* and *in vitro*. Further studies on the mechanism of CGA with regard to anti-liver fibrosis may help to find a new way to prevent and treat schistosome-induced hepatic fibrosis.

MATERIALS AND METHODS

Chemicals and reagents. Chlorogenic acid (≥95% titration) was purchased from Sigma-Aldrich (Switzerland). RPMI 1640 medium, basic and with fetal bovine serum (FBS), was purchased from Gibco (Grand Island, NY, USA). IL-13 was purchased from Peprotech (Rocky Hill, NJ, USA). CCK8 was purchased from Dojindo Laboratories (Japan). Rabbit anti-mouse Smad7, CTGF, Smad1, p-Smad1, Smad2, p-Smad2, Smad2/3, p-Smad2/3, TGF-β receptor I, and α-SMA antibodies were obtained from Cell Signaling Technology (CST) (Boston, MA, USA). Biotin-conjugated goat anti-rabbit IgG and streptavidin-horseradish peroxidase (HRP) conjugate were obtained from Wuhan Boster Biotechnology Co., Ltd. (Wuhan, China). RNAiso Plus, the PrimeScript RT reagent kit, and the SYBR Premix *Ex Taq* kit were purchased from TaKaRa (Dalian, China). The miR-21 and negative-control lentiviral vectors were constructed by GeneChem Co., Ltd. (Shanghai, China).

Cell culture, cytokine and chemical treatment, and cytotoxic effect of CGA. RPMI 1640 medium mixed with 10% FBS was used to culture LX2 cells in an incubator at 37°C, 5% CO_2, and saturated humidity (38, 39). Human recombinant IL-13 (rIL-13) was used for cellular-model establishment. The intervention groups were divided into a control group, an IL-13 experimental group, and CGA (20-μg/ml, 40-μg/ml, and 80-μg/ml) groups. After the cells were passaged in 6-well plates (for real-time PCR and Western blotting) or 96-well plates (for CCK8 experiments and preliminary lentiviral transfection experiments) for 24 h and cultured to 70% density, the supernatants were removed and CGA was diluted in RPMI 1640 medium to concentrations of 20 μg/ml, 40 μg/ml, and 80 μg/ml for interfering with the cells, excluding the control and IL-13 experimental groups. In the final 6 h, IL-13 (50 ng/ml) was added to the wells for modeling, except for the control group. After 24 h, the supernatants and cells were harvested. Cells stimulated with IL-13 without any intervention were observed as the IL-13 experimental group, whereas cells incubated in RPMI 1640 medium alone served as the control group. The cytotoxic effect of CGA was evaluated by CCK8 assay.

Knockdown and overexpression of miR-21. For knockdown, the sequence of hsa-miR-21-3p inhibition (vector no. 16129-1) was 5′-TCGAGAAAAAACAGCCCATCGACTGGTGTTGTTTTTC-3′, and the reference sequence was 5′-TTCTCCGAACGTGTCACGT-3′. GV369–miR-21/NC–enhanced green fluorescent protein (EGFP) was transfected into the 293 T cell line, and the viral supernatant was harvested after 48 h (5×10^8 transducing units [TU]/ml). For overexpression, GV273–miR-21/NC–EGFP was transfected into the 293 T cell line, and the viral supernatant was harvested after 48 h (3×10^8 TU/ml). LX2 cells were seeded onto 24- or 12-well plates and transfected with lentivirus at a multiplicity of infection (MOI) of 10 according to the manufacturer's instructions. The medium was replaced 12 h later, and the cells were grown for an additional time up to 72 h. Knockdown or overexpression of miR-21 was confirmed by real-time PCR analysis.

Animal groups. Fifty male BALB/c mice weighing 18 to 22 g were purchased from the Hubei Provincial Center for Disease Control and Prevention (Wuhan, China). The mice were maintained as we described previously (40). All study protocols were in accordance with internationally accepted principles and the Guidelines for the Care and Use of Laboratory Animals of Huazhong University of Science and Technology, Wuhan, People's Republic of China. The animal experiment number was SCXK(HUBEI) 2015-0018. The study was reviewed and approved by the Research Ethics Committee of Tongji Medical College, Huazhong University of Science and Technology (IORG no. IORG0003571). The mice were divided into 5 equal groups: CGA low concentration (5 mg/kg of body weight), CGA medium concentration (10 mg/kg), CGA high concentration (20 mg/kg), experimental, and control groups. All groups except the control group were infected with 25 ± 5 *Schistosoma japonicum* cercaria (Fig. 8B) by the abdominal-patch method (41). At the end of 4 weeks of infection, the mice in the experimental and CGA groups were administered praziquantel (500 mg/kg) for 5 days, while in the control group, normal saline was used instead of praziquantel. Then, the mice in the experimental and control groups were administered normal saline and the mice in the three CGA groups were administered CGA at 5 mg/kg, 10 mg/kg, or 20 mg/kg for 4 weeks.

Specimen collection and liver histological studies. After administration, the mice in each group were euthanized to collect specimens. The procedure matched that of our past experiment (42, 43). The procedures of the H&E and Sirius red staining assays followed the previously described steps (44, 45). A fresh liver specimen was fixed in 10% neutral buffered formalin for 3 days and then embedded in paraffin for histological examinations. Sections (5 μm) were cut with a Leica SM2010 R sliding microtome (Shanghai, China) and stained with H&E or Sirius red to assess liver damage and fibrosis development. The paraffin-embedded tissues were cut into 4-μm slices and deparaffinated in dimethylbenzene for 5 to 10 min. Then, the tissues were put into 100%, 95%, 85%, and 70% alcohol for 2 to 5 min in turn and finally washed with distilled water and immersed in the staining solution. After hematoxylin staining for 5 to 15 min, the excess stain solution on the slides was washed off, and color separation with 0.5 to 1% hydrochloride alcohol (made from 75% alcohol) was performed for about 10 s. Following washing with running water for 15 to 30 min, the tissues were stained with 0.1 to 0.5% eosin for 1 to 5 min. Prior to being hyalinized with dimethylbenzene twice for about 10 min in total, the tissues were dehydrated with 75%, 85%, 95%, and 100% alcohol for 2 to 3 min in turn. Finally, a few drops of neutral gum were added to the coverslip and covered by a slide. Histological changes were evaluated by analyzing five nonconsecutive and random histological fields at $\times$400 magnification.

ELISA to measure IL-13 in serum. The enzyme-linked immunosorbent assay (ELISA) procedure was based on our past experiments (46, 47). The IL-13 produced by mice was determined by sandwich ELISA. Sera were assayed with IL-13 ELISA kits. The procedure was in accordance with the instruction manuals of the respective kits.

Quantitative real-time PCR to detect mRNA expression. The PCR procedure followed the previously published steps (48). Total RNA in BV2 cells was isolated by using RNAiso Plus according to the manufacturer's protocol. The cDNAs were produced with a PrimeScript RT reagent kit and incubated at 37°C for 15 min and 85°C for 5 s. Real-time PCRs were performed using a StepOne Plus device (Applied Biosystems) at 95°C for 10 s, followed by 40 cycles of 95°C for 5 s and 60°C for 20 s, according to the instructions for the SYBR Premix *Ex Taq* kit. The data were analyzed by the $2^{-\Delta\Delta CT}$ method (49). All the primers were synthesized by GenScript (Nanjing, China), and the sequences are shown in Table 1.

Western blotting for protein expression measurement. The Western blotting procedure followed the previously published steps (50). Western blots were carried out using whole-cell extracts separated on SDS-PAGE gels and then transferred onto a nitrocellulose filter membrane. The membranes were blocked overnight with 5% nonfat milk in phosphate-buffered saline (PBS) and probed with the indicated antibody (Ab) before being washed three times in Tris-buffered saline with Tween 20 (TBST) and then

TABLE 1 Primer sequences for real-time quantitative PCR

Gene	Primer	Sequence (5′→3′)	
		Human	Mouse
miR-21	RT stem-loop	CTCAACTGGTGTCGTGGAGTCGGCAATTCAGTTGAGTCAACATC	GTCGTATCCAGTGCAGGGTCCGAGGTATTCGCACTGGATACGACTCAACATC
	Forward	ACACTCCAGCTGGGTAGCTTATCAGACTGA	ATGGTTCGTGGGTAGCTTATCAGACTGA
	Reverse	TGGTGTCGTGGAGTCG	GCAGGGTCCGAGGTATTC
Smad7	Forward	AGAGGCTGTGTTGCTGTGAAT	GTGTTGCTGTGAATCTTACG
	Reverse	GCAGAGTCGGCTAAGGTGATG	AGAAGAAGTTGGGAATCTGA
CTGF	Forward	AATGCTGCGAGGAGTGGGT	TCAACCTCAGACACTGGTTTCG
	Reverse	CGGCTCTAATCATAGTTGGGTCT	TAGAGCAGGTCTGTCTGCAAGC
GAPDH	Forward	ACCACAGTCCATGCCATCAC	ACCACAGTCCATGCCATCAC
	Reverse	TCCACCACCCTGTTGCTGTA	TCCACCACCCTGTTGCTGTA

incubated with an HRP-labeled secondary Ab. The dilutions of the primary and secondary antibodies were as follows: Smad7, 1:800; CTGF, 1:1,000; Smad1, 1:1,000; p-Smad1, 1:1,000; Smad2, 1:1,000; Smad2/3, 1:1,000; p-Smad2/3, 1:1,000; TGF-β receptor I, 1:500; α-SMA, 1:1,000; and GAPDH (glyceraldehyde-3-phosphate dehydrogenase), 1:5,000. After further washing with TBST, enhanced chemiluminescence (ECL) was used to identify immunoreactive bands. Densitometry analysis of the immunoreactive bands was performed using the Fuji ultrasonic-Doppler velocity profile (UVP) system and the ImageJ program.

IHC to detect α-SMA expression in liver tissue. The IHC procedure followed that of our previous experiment (51). The liver tissue specimens were cut into 10-μm sections after dewaxing and hydrating. The sections were incubated in 3% H_2O_2-methanol to eliminate endogenous peroxidase activity. Then, the sections were incubated with normal goat serum for 10 min and incubated with α-SMA antibody (1:400) overnight at 4°C and biotinylation secondary antibody at 37°C for 45 min. They were rinsed again with PBS and incubated with horseradish peroxidase-labeled streptavidin at 37°C. The samples were developed with diaminobenzidine (DAB) and stained with hematoxylin. After being rinsed with distilled water and dehydrated, the sections were made transparent and mounted for microscope examination. After the immunohistochemical analysis, Image-Pro Plus 6.0 (IPP) software was used to analyze the optical density of the images, as described previously.

Statistical analysis. All statistical analyses were performed with SPSS 12.0. The results were expressed as means and standard errors of the mean (SEM). Comparisons of the measurement data between groups were performed with Student's *t* test and one-way analysis of variance (ANOVA). A *P* value of <0.05 was considered statistically significant (52).

ACKNOWLEDGMENTS

We have no potential conflicts of interest to disclose.

This study was supported by the National Natural Science Foundation of China (no. 81371840).

REFERENCES

1. Wu J, Xu W, Ming Z, Dong H, Tang H, Wang Y. 2010. Metabolic changes reveal the development of schistosomiasis in mice. PLoS Negl Trop Dis 4:e807. https://doi.org/10.1371/journal.pntd.0000807.
2. Ali SA, El-Regal NS, Saeed SM. 2015. Antischistosomal activity of two active constituents isolated from the leaves of Egyptian medicinal plants. Infect Dis (Auckl) 8:5–16. https://doi.org/10.4137/IDRT.S24342.
3. Colley DG, Bustinduy AL, Secor WE, King CH. 2014. Human schistosomiasis. Lancet 383:2253–2264. https://doi.org/10.1016/S0140-6736(13)61949-2.
4. Ross AG, Olveda RM, Acosta L, Harn DA, Chy D, Li Y, Gray DJ, Gordon CA, McManus DP, Williams GM. 2013. Road to the elimination of schistosomiasis from Asia: the journey is far from over. Microbes Infect 15:858–865. https://doi.org/10.1016/j.micinf.2013.07.010.
5. Thétiot-Laurent SA, Boissier J, Robert A, Meunier B. 2013. Schistosomiasis chemotherapy. Angew Chem Int Ed Engl 52:7936–7956. https://doi.org/10.1002/anie.201208390.
6. Wang W, Wang L, Liang YS. 2012. Susceptibility or resistance of praziquantel in human schistosomiasis: a review. Parasitol Res 111:1871–1877. https://doi.org/10.1007/s00436-012-3151-z.
7. Liu Y, Meyer C, Müller A, Herweck F, Li Q, Müllenbach R, Mertens PR, Dooley S, Weng HL. 2011. IL-13 induces connective tissue growth factor in rat hepatic stellate cells via TGF-β-independent Smad signaling. J Immunol 187:2814–2823. https://doi.org/10.4049/jimmunol.1003260.
8. Denecke B, Wickert L, Liu Y, Ciuclan L, Dooley S, Meindl-Beinker NM. 2010. Smad7 dependent expression signature highlights BMP2 and HK2 signaling in HSC transdifferentiation. World J Gastroenterol 16:5211–5224. https://doi.org/10.3748/wjg.v16.i41.5211.
9. Boerjan W, Ralph J, Baucher M. 2003. Lignin biosynthesis. Annu Rev Plant Biol 54:519–546. https://doi.org/10.1146/annurev.arplant.54.031902.134938.
10. Gao R, Lin Y, Liang G, Yu B, Gao Y. 2014. Comparative pharmacokinetic study of chlorogenic acid after oral administration of Lonicerae Japonicae Flos and Shuang-Huang-Lian in normal and febrile rats. Phytother Res 28:144–147. https://doi.org/10.1002/ptr.4958.
11. Kweon MH, Hwang HJ, Sung HC. 2001. Identification and antioxidant activity of novel chlorogenic acid derivatives from bamboo (Phyllostachys edulis). J Agric Food Chem 49:4646–4655. https://doi.org/10.1021/jf010514x.
12. Nicasio P, Aguilar-Santamaría L, Aranda E, Ortiz S, González M. 2005. Hypoglycemic effect and chlorogenic acid content in two Cecropia species. Phytother Res 19:661–664. https://doi.org/10.1002/ptr.1722.
13. Guo YJ, Luo T, Wu F, Mei YW, Peng J, Liu H, Li HR, Zhang SL, Dong JH, Fang Y, Zhao L. 2015. Involvement of TLR2 and TLR9 in the anti-inflammatory effects of chlorogenic acid in HSV-1-infected microglia. Life Sci 127:12–18. https://doi.org/10.1016/j.lfs.2015.01.036.
14. Riksen NP, Rongen GA, Smits P. 2009. Acute and long-term cardiovascular effects of coffee: implications for coronary heart disease. Pharmacol Ther 121:185–191. https://doi.org/10.1016/j.pharmthera.2008.10.006.
15. Shibata H, Sakamoto Y, Oka M, Kono Y. 1999. Natural antioxidant, chlorogenic acid, protects against DNA breakage caused by monochloramine. Biosci Biotechnol Biochem 63:1295–1297. https://doi.org/10.1271/bbb.63.1295.
16. Zhao Y, Wang J, Ballevre O, Luo H, Zhang W. 2012. Antihypertensive effects and mechanisms of chlorogenic acids. Hypertens Res 35:370–374. https://doi.org/10.1038/hr.2011.195.
17. Granado-Serrano AB, Martín MA, Izquierdo-Pulido M, Goya L, Bravo L, Ramos S. 2007. Molecular mechanisms of (−)-epicatechin and chlorogenic acid on the regulation of the apoptotic and survival/proliferation pathways in a human hepatoma cell line. J Agric Food Chem 55:2020–2027. https://doi.org/10.1021/jf062556x.
18. Jiang Y, Kusama K, Satoh K, Takayama E, Watanabe S, Sakagami H. 2000. Induction of cytotoxicity by chlorogenic acid in human oral tumor cell lines. Phytomedicine 7:483–491. https://doi.org/10.1016/S0944-7113(00)80034-3.
19. dos Santos MD, Almeida MC, Lopes NP, de Souza GE. 2006. Evaluation of the anti-inflammatory, analgesic and antipyretic activities of the natural polyphenol chlorogenic acid. Biol Pharm Bull 29:2236–2240. https://doi.org/10.1248/bpb.29.2236.
20. Takahama U, Tanaka M, Hirota S. 2008. Interaction between ascorbic acid and chlorogenic acid during the formation of nitric oxide in acidified saliva. J Agric Food Chem 56:10406–10413. https://doi.org/10.1021/jf8018535.
21. Shen W, Qi R, Zhang J, Wang Z, Wang H, Hu C, Zhao Y, Bie M, Wang Y, Fu Y, Chen M, Lu D. 2012. Chlorogenic acid inhibits LPS-induced microglial activation and improves survival of dopaminergic neurons. Brain Res Bull 88:487–494. https://doi.org/10.1016/j.brainresbull.2012.04.010.
22. Shi H, Dong L, Bai Y, Zhao J, Zhang Y, Zhang L. 2009. Chlorogenic acid against carbon tetrachloride-induced liver fibrosis in rats. Eur J Pharmacol 623:119–124. https://doi.org/10.1016/j.ejphar.2009.09.026.
23. Shi H, Dong L, Jiang J, Zhao J, Zhao G, Dang X, Lu X, Jia M. 2013. Chlorogenic acid reduces liver inflammation and fibrosis through inhibition of Toll-like receptor 4 signalling pathway. Toxicology 303:107–114. https://doi.org/10.1016/j.tox.2012.10.025.
24. Shi H, Shi A, Dong L, Lu X, Wang Y, Zhao J, Dai F, Guo X. 2016. Chlorogenic acid protects against liver fibrosis in vivo and in vitro

through inhibition of oxidative stress. Clin Nutr. https://doi.org/10.1016/j.clnu.2016.03.002.
25. Chuah C, Jones MK, Burke ML, McManus DP, Gobert GN. 2014. Cellular and chemokine-mediated regulation in schistosome-induced hepatic pathology. Trends Parasitol 30:141–150. https://doi.org/10.1016/j.pt.2013.12.009.
26. Barron L, Wynn TA. 2011. Macrophage activation governs schistosomiasis-induced inflammation and fibrosis. Eur J Immunol 41:2509–2514. https://doi.org/10.1002/eji.201141869.
27. He X, Xie J, Zhang D, Su Q, Sai X, Bai R, Chen C, Luo X, Gao G, Pan W. 2015. Recombinant adeno-associated virus-mediated inhibition of microRNA-21 protects mice against the lethal schistosome infection by repressing both IL-13 and transforming growth factor beta 1 pathways. Hepatology 61:2008–2017. https://doi.org/10.1002/hep.27671.
28. Sombetzki M, Loebermann M, Reisinger EC. 2015. Vector-mediated microRNA-21 silencing ameliorates granulomatous liver fibrosis in Schistosoma japonicum infection. Hepatology 61:1787–1789. https://doi.org/10.1002/hep.27748.
29. Gressner OA, Lahme B, Demirci I, Gressner AM, Weiskirchen R. 2007. Differential effects of TGF-beta on connective tissue growth factor (CTGF/CCN2) expression in hepatic stellate cells and hepatocytes. J Hepatol 47:699–710. https://doi.org/10.1016/j.jhep.2007.05.015.
30. Gressner OA, Gressner AM. 2008. Connective tissue growth factor: a fibrogenic master switch in fibrotic liver diseases. Liver Int 28:1065–1079. https://doi.org/10.1111/j.1478-3231.2008.01826.x.
31. Hernandez-Gea V, Friedman SL. 2011. Pathogenesis of liver fibrosis. Annu Rev Pathol 6:425–456. https://doi.org/10.1146/annurev-pathol-011110-130246.
32. Uesugi T, Froh M, Arteel GE, Bradford BU, Thurman RG. 2001. Toll-like receptor 4 is involved in the mechanism of early alcohol-induced liver injury in mice. Hepatology 34:101–108. https://doi.org/10.1053/jhep.2001.25350.
33. Van Hul NK, Abarca-Quinones J, Sempoux C, Horsmans Y, Leclercq IA. 2009. Relation between liver progenitor cell expansion and extracellular matrix deposition in a CDE-induced murine model of chronic liver injury. Hepatology 49:1625–1635. https://doi.org/10.1002/hep.22820.
34. Huang Y, Yang YB, Zhang XH, Yu XL, Wang ZB, Cheng XC. 2013. MicroRNA-21 gene and cancer. Med Oncol 30:376. https://doi.org/10.1007/s12032-012-0376-8.
35. Li S, Liang Z, Xu L, Zou F. 2012. MicroRNA-21: a ubiquitously expressed pro-survival factor in cancer and other diseases. Mol Cell Biochem 360:147–158. https://doi.org/10.1007/s11010-011-1052-6.
36. Maemura K, Natsugoe S, Takao S. 2014. Molecular mechanism of cholangiocarcinoma carcinogenesis. J Hepatobiliary Pancreat Sci 21:754–760. https://doi.org/10.1002/jhbp.126.
37. Jiang H, Wu W, Zhang M, Li J, Peng Y, Miao TT, Zhu H, Xu G. 2014. Aberrant upregulation of miR-21 in placental tissues of macrosomia. J Perinatol 34:658–663. https://doi.org/10.1038/jp.2014.58.
38. Zhao L, Tao JY, Zhang SL, Jin F, Pang R, Dong JH. 2010. *N*-Butanol extract from Melilotus suaveolens Ledeb affects pro- and anti-inflammatory cytokines and mediators. Evid Based Complement Alternat Med 7:97–106. https://doi.org/10.1093/ecam/nem165.
39. Jin F, Gao C, Zhao L, Zhang H, Wang HT, Shao T, Zhang SL, Wei YJ, Jiang XB, Zhou YP, Zhao HY. 2011. Using CD133 positive U251 glioblastoma stem cells to establish nude mice model of transplanted tumor. Brain Res 1368:82–90. https://doi.org/10.1016/j.brainres.2010.10.051.
40. Guo YJ, Luo T, Wu F, Liu H, Li HR, Mei YW, Zhang SL, Tao JY, Dong JH, Fang Y, Zhao L. 2015. Corilagin protects against HSV1 encephalitis through inhibiting the TLR2 signaling pathways in vivo and in vitro. Mol Neurobiol 52:1547–1560. https://doi.org/10.1007/s12035-014-8947-7.
41. Yang F, Wang Y, Xue J, Ma Q, Zhang J, Chen YF, Shang ZZ, Li QQ, Zhang SL, Zhao L. 2016. Effect of corilagin on the miR-21/smad7/ERK signaling pathway in a schistosomiasis-induced hepatic fibrosis mouse model. Parasitol Int 65:308–315. https://doi.org/10.1016/j.parint.2016.03.001.
42. Jin F, Cheng D, Tao JY, Zhang SL, Pang R, Guo YJ, Ye P, Dong JH, Zhao L. 2013. Anti-inflammatory and anti-oxidative effects of corilagin in a rat model of acute cholestasis. BMC Gastroenterol 13:79. https://doi.org/10.1186/1471-230X-13-79.
43. Li HR, Li G, Li M, Zhang SL, Wang H, Luo T, Wu F, Dong JH, Guo YJ, Zhao L. 2016. Corilagin ameliorates schistosomiasis hepatic fibrosis through regulating IL-13 associated signal pathway in vitro and in vivo. Parasitology 143:1629–1638. https://doi.org/10.1017/S0031182016001128.
44. Huang YF, Zhang SL, Jin F, Cheng D, Zhou YP, Li HR, Tang ZM, Xue J, Cai W, Dong JH, Zhao L. 2013. Activity of corilagin on post-parasiticide liver fibrosis in schistosomiasis animal model. Int J Immunopathol Pharmacol 26:85–92. http://journals.sagepub.com/doi/abs/10.1177/039463201302600108.
45. Chen L, Li L, Chen J, Li L, Zheng Z, Ren J, Qiu Y. 2015. Oleoylethanolamide, an endogenous PPAR-α ligand, attenuates liver fibrosis targeting hepatic stellate cells. Oncotarget 6:42530–42540. https://doi.org/10.18632/oncotarget.6466.
46. Li XF, Guo YJ, Zhang DM, Chen Z, Wei X, Li YH, Zhang SL, Tao JY, Dong JH, Mei YW, Li LL, Zhao L. 2012. Protective activity of the ethanol extract of Cynanchum paniculatum (BUNGE) Kitagawa on treating herpes simplex encephalitis. Int J Immunopathol Pharmacol 25:259–266. http://journals.sagepub.com/doi/abs/10.1177/039463201202500128.
47. Li XF, Guo YJ, Wang ML, Zhang DM, Li YH, Wang YF, Tao JY, Zhang SL, Dong JH, Li LL, Zhao L. 2011. Inducing-apoptotic activity of the ethanol extract of Duchesnea indica Focke on treatment of herpes simplex encephalitis. Int J Immunopathol Pharmacol 24:631–638. http://journals.sagepub.com/doi/abs/10.1177/039463201102400309.
48. Zhou YP, Cheng D, Zhang SL, Li HR, Tang ZM, Xue J, Cai W, Dong JH, Zhao L. 2013. Preliminary exploration on anti-fibrosis effect of kaempferol in mice with Schistosoma japonicum infection. Eur J Inflamm 11:161–168. http://journals.sagepub.com/doi/abs/10.1177/1721727X1301100115.
49. Schmittgen TD, Livak KJ. 2008. Analyzing real-time PCR data by the comparative C(T) method. Nat Protoc 3:1101–1108. https://doi.org/10.1038/nprot.2008.73.
50. Zhao L, Zhang SL, Tao JY, Jin F, Pang R, Guo YJ, Ye P, Dong JH, Zheng GH. 2008. Anti-inflammatory mechanism of a folk herbal medicine, Duchesnea indica (Andr) Focke at RAW264.7 cell line. Immunol Invest 37:339–357. https://doi.org/10.1080/08820130802111589.
51. Jin F, Zhang R, Feng S, Yuan CT, Zhang RY, Han GK, Li GH, Yu XZ, Liu Y, Kong LS, Zhang SL, Zhao L. 2015. Pathological features of transplanted tumor established by CD133 positive TJ905 glioblastoma stem-like cells. Cancer Cell Int 15:60. https://doi.org/10.1186/s12935-015-0208-y.
52. Ding Y, Li G, Xiong LJ, Yin W, Liu J, Liu F, Wang RG, Xia K, Zhang SL, Zhao L. 2015. Profiles of responses of immunological factors to different subtypes of Kawasaki disease. BMC Musculoskelet Disord 16:315. https://doi.org/10.1186/s12891-015-0744-6.